

## Quantum hard spheres in a channel\*

K. S. Liu<sup>†</sup> and M. H. Kalos<sup>†</sup>

*Courant Institute, New York University, New York, New York 10012*

G. V. Chester

*Laboratory of Atomic and Solid State Physics, Cornell University, Ithaca, New York 14850*

(Received 12 March 1974)

A quantum hard-sphere system bounded by two parallel rigid walls is studied at absolute zero by numerically integrating the Schrödinger equation for the system. A very pronounced layered structure in the density profile across the channel is observed. The numerical calculations are performed on fairly small systems of about 64 hard spheres. It is also found that the layered structure is very sensitive to the distance between the walls. A comparison is made with the results of variational calculations which also show definite but less striking layered structures. A classical hard-sphere fluid in a similar geometry again shows a layered structure which is also sensitive to the distance between the walls. We suggest that the occurrence of the layers can be semiquantitatively related to the oscillations exhibited by the radial distribution function at the same density.

### I. INTRODUCTION

Many experiments<sup>1</sup> have been conducted in an effort to understand boundary and size effects on the properties of liquid <sup>4</sup>He. These experiments have yielded some understanding of the effects introduced either by a substrate or the walls of a narrow channel. A difficulty in interpreting the experiments is that up to the present no accurate calculations of the structure and properties of helium near a substrate or wall were available. A very simple model of the density profile was introduced some years ago.<sup>2</sup> This assumes that some kind of step-wise density profile is appropriate near a substrate. To study the behavior of the order parameter, the Hartree approximation has often been used.<sup>3</sup> Since both these models are based on very crude approximations their reliability as an aid to interpreting data is considerably in doubt. The main purpose of this paper is to present the results of an essentially exact calculation of the density profile of a fluid boson system in a narrow channel. The model we use, namely, hard spheres between parallel hard walls, is highly idealized and we view these calculations as being exploratory. Nevertheless, we have found some striking results which we believe will be present in a more realistic model.

A recent paper demonstrates that the local spatial structure (as revealed by the radial distribution function) in a uniform system of bosons can be very accurately represented by a hard-sphere model for the fluid<sup>4</sup> (hereafter referred to as I). Indeed, at the appropriate density the

structure factor for the hard-sphere system is almost identical with that measured by x-ray scattering on liquid helium. Because the local structure is so well represented by the hard-sphere model, we feel that the use of the same model to represent liquid helium confined in a narrow channel is a good first approximation. We, of course, shall emphasize the structure of the fluid. Questions relating to the binding of the fluid to the substrate and the flow of the fluid over a rough substrate require a much more realistic model.

In a previous publication<sup>5</sup> (hereafter referred to as II) we presented the results of a variational calculation using Monte Carlo methods. It was found that for the same model of hard spheres in a channel that the density profile across the channel exhibits a layered structure. The loose analogy between the density profile and the radial distribution function in a uniform system was pointed out. In the variational calculation the order parameter also showed considerable structure. We argued in II that the oscillatory behavior was expected, although it could also be argued that it arose from the functional form of the trial variational wave function. The results of the exact calculations which we present in this paper show even more enhanced density oscillations than those revealed by the variational calculations, thus verifying that they are not an artifact of the variational approach.

The exact calculation is based on a numerical method proposed by one of the present authors<sup>6</sup> and recently applied in I to a uniform system of hard-sphere bosons. The methods can give exact

numerical results for the properties of hard-sphere systems. The numerical methods used for the channel problem are fundamentally the same as those in I and the reader is referred to that paper for basic details.

In Sec. II the numerical method as modified, for the present study, is briefly described with emphasis placed on the changes needed for this problem as compared with the work reported in I. Our results are presented in Sec. III. Some of the results found were so striking that we were led to investigate, for purposes of comparison, a similar system of classical hard spheres in a channel. This comparison is made in Sec. IV. Section V is devoted to a discussion of whether our system finally reached a true equilibrium state. This is an important question in this kind of numerical work. The numerical experiments we conducted show quite convincingly that we did, indeed, achieve equilibrium. Section VI is devoted to our conclusions and discussion of future work.

## II. HARD-SPHERE MODEL

$N$  hard spheres are enclosed in a rectangular box  $L_x \times L_y \times L_z$ . Periodic extensions are made in the  $x$  and  $y$  directions. The surfaces at  $z=0$  and  $z=L_z$  are assumed to be rigid repulsive walls. The Schrödinger equation for this system is (with  $\hbar = 2m = 1$ , and hard-sphere diameter  $= a$ )

$$-\nabla^2 \psi(R) = E \psi(R), \quad (1)$$

with the boundary conditions

$$\psi(R) = 0 \quad \text{if } |\vec{r}_i - \vec{r}_j| \leq a \text{ for all } i \neq j \quad (2a)$$

or

$$z_i \leq 0 \quad \text{or} \quad z_i \geq L_z \quad \text{for all } i, \quad (2b)$$

where  $R$  stands for  $3N$  particle coordinates  $\{\vec{r}_1, \vec{r}_2, \dots, \vec{r}_N\}$ , and  $\vec{r}_i = (x_i, y_i, z_i)$ . If we define  $G(R, R_0)$  through

$$-\nabla^2 G(R, R_0) = \delta(R - R_0), \quad (3)$$

then Eq. (1) may be rewritten as

$$\psi(R) = E \int G(R, R') \psi(R') dR'. \quad (4)$$

If  $\psi_J(R)$  is a trial function for importance sampling, and if

$$\tilde{\psi}(R) = \psi_J(R) \psi(R), \quad (5)$$

then Eq. (4) may be transformed to

$$\tilde{\psi}(R) = E \int [\psi_J(R) G(R, R') \psi_J^{-1}(R')] \tilde{\psi}(R') dR' \equiv Y \tilde{\psi}. \quad (6)$$

It was demonstrated in paper I that if  $\psi_J(R)$  is the exact ground-state wave function, then the method using important sampling with  $\psi_J(R)$  will give zero variances in estimation of ground-state energy. When  $\psi_J(R)$  is a good approximate ground-state wave function, the convergence will be accelerated. For the present purpose, we choose the optimal variational wave function we found in paper II, i.e.,

$$\psi_J(R) = \left( \prod_{i < j} f_{ij} \right) \prod_k h(z_k), \quad (7a)$$

where

$$f(r) = \tanh[(r^m - 1)/b^m], \quad (7b)$$

$$h(z) = h_0(z) = \tanh[z(L_z - z)/dL_z]^q. \quad (7c)$$

The main differences between the present calculation and that in I are given by Eqs. (2b) and (7) and the removal of the periodic extension in the  $z$  direction. These differences can be incorporated into the methods of I. For details on how the solution of Eq. (6) is found, readers should consult I.

From the solution of Eq. (6), one has a statistical sample whose population is proportional to  $\psi_J(R) \psi_0(R)$ ,  $\psi_0(R)$  being the "exact" ground-state wave function. To calculate expectation values weighted with  $\psi_0^2(R)$ , one may use the following scheme.

Suppose  $\{\psi_k\}$  is a complete set of eigenfunctions of Eq. (4) with eigenvalues  $E_k$ . Then one has the completeness relation among them

$$\sum_k \psi_k^*(R) \psi_k(R') = \delta(R - R'). \quad (8)$$

This can be written as

$$\sum_k \frac{\psi_k^*(R)}{\psi_J(R)} \psi_k(R') \psi_J(R) = \delta(R - R'). \quad (9)$$

If we apply the operator  $Y$  defined in Eq. (6) to Eq. (9)  $m$  times and integrate both sides over  $R'$ , then in the limit  $m \rightarrow \infty$ , one obtains

$$\begin{aligned} q(R) &= \lim_{m \rightarrow \infty} \int Y^m \delta(R - R') dR' \\ &= \lim_{m \rightarrow \infty} \sum_k \frac{\psi_k^*(R)}{\psi_J(R)} \int Y^m \tilde{\psi}_k(R') dR', \\ &= \lim_{m \rightarrow \infty} \sum_k \frac{\psi_k^*(R)}{\psi_J(R)} \left( \frac{E}{E_k} \right)^m \int \tilde{\psi}_k(R') dR' \propto \frac{\psi_0(R)}{\psi_J(R)}. \end{aligned} \quad (10)$$

Let  $\{R_I\}$  be a population drawn from  $\psi_J(R) \psi_0(R)$ . Use  $q(R_I)$ , the asymptotic population obtained from iteration starting with  $R_I$ , as the weight. Then the density of the weight occurring in the neighborhood

of  $R_i$  will be proportional to  $[\psi_0(R)/\psi_J(R)]\psi_J(R) \times \psi_0(R) = \psi_0^2(R)$ . From this distribution one readily obtains the density profile defined by

$$n(\bar{r}) = \frac{N \int \psi_0^2(R) \delta(\bar{r} - \bar{r}_1) dR}{\int \psi_0^2(R) dR}. \quad (11)$$

A subscript  $m$  will be attached if the weights are obtained from Eq. (10) after  $m$  iterations.

For practical purposes, it is also useful to compute average weighted with  $\psi_J(R)\psi_0(R)$ :

$$n_J(\bar{r}) = \frac{N \int \psi_0(R)\psi_J(R)\delta(\bar{r} - \bar{r}_1) dR}{\int \psi_0(R)\psi_J(R) dR}. \quad (12)$$

It can be seen that  $n_J(r)$  is an intermediate quantity between the "exact"  $n(r)$  and that obtained from a variational result,  $n_v(r)$  computed from  $\psi_J^2(R)$ . For clarity we shall keep these labels on the density profiles whenever necessary.

In contrast to the bulk calculations reported in I, we find some striking quantitative changes between the variational results and those obtained from integrating the Schrödinger equation. This means that our trial function for the channel problem is not as good here as those used in the bulk fluid. It also implies that the convergence required in Eq. (10) is slower and subject to more statistical error than for the bulk. However, by comparing results of  $n_m$  and  $n_{2m}$ , we can estimate possible uncertainties for these weights. We find

that the difference between  $n_{40}$  and  $n_{80}$  is very much less than the difference between either of these functions and  $n_v$  obtained from a variational calculation. Next the difference between  $n_{40}$  or  $n_{80}$  and  $n_J$  is about 1–2%, which is very much less than the 10–15% difference between  $n_J$  and  $n_v$  (this is shown clearly in Figs. 1 and 2). In other words,  $n_{40}$ ,  $n_{80}$ , and  $n_J$  are all very close to one another, and differ appreciably from  $n_v$ . Since  $n_J$  can be computed comparatively easily, we shall confine our attention to the function for most of our analysis.

### III. RESULTS FOR QUANTUM HARD SPHERES

In Figs. 2–4, density profiles  $n_J(z)$  are plotted for three different channel widths:  $L_{z1} = L_0 = 6.84a$ ;  $L_{z2} = \frac{31}{32}L_0$ ;  $L_{z3} = \frac{15}{16}L_0$ . The average density is kept at  $\rho a^3 = 0.2$ . This is equivalent to a density of  $\rho \sigma^3 = 0.34$  in liquid helium. For comparison, the results of our variational calculations  $n_v(z)$  are also included.

We point out two striking features in these graphs. Firstly, a layered structure exists in both the exact and variational calculations, but the layers are much more pronounced and are damped out more slowly in the exact treatment. This is especially true for the layers in the middle of the channel. Secondly, as the channel width is reduced, the middle layer disappears for  $L_z = L_{z2}$

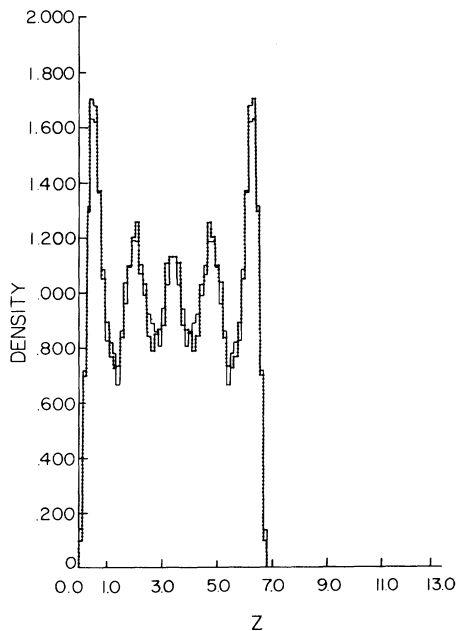


FIG. 1. Density profiles for quantum hard spheres in a channel for the density  $\rho a^3 = 0.2$  and the channel width  $L_z = L_{z0} = 6.84a$ ,  $n_{40}(z)/\rho$ , the solid line decorated with dots, and  $n_J(z)/\rho$  the undecorated solid line. See the text for definitions of  $n_{40}(z)$  and  $n_J(z)$ .

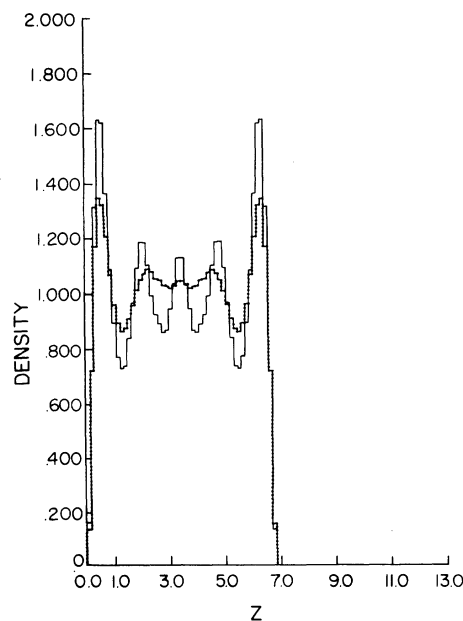


FIG. 2. Density profiles for quantum hard spheres for  $\rho a^3 = 0.2$  and  $L_z = L_{z0}$ . The solid line is  $n_J(z)/\rho$  from the present treatment. The decorated line for  $n_v(z)/\rho$  is from the variational calculation.

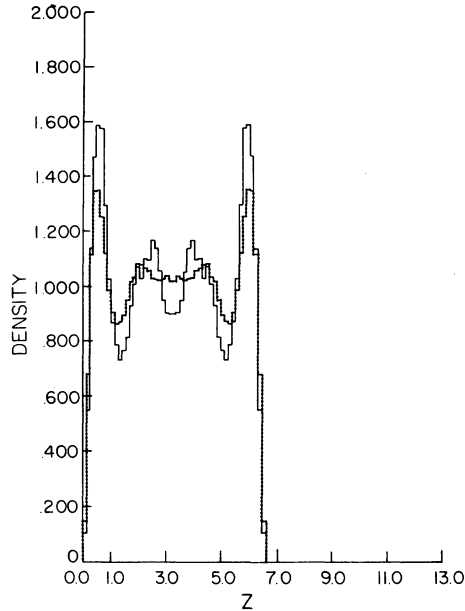


FIG. 3. Density profiles for quantum hard spheres for  $\rho a^3 = 0.2$  and  $L_z = \frac{31}{32} L_{z0}$ . The solid line for  $n_J(z)/\rho$  is from the present treatment. The decorated line for  $n_v(z)/\rho$  is from the variational calculation.

and  $L_z = L_{z3}$ . As the number of layers drops for these separations, the second layers from the walls tend to increase their peak heights and at the same time the layers are slightly broadened. In the variational treatment, any such sensitive

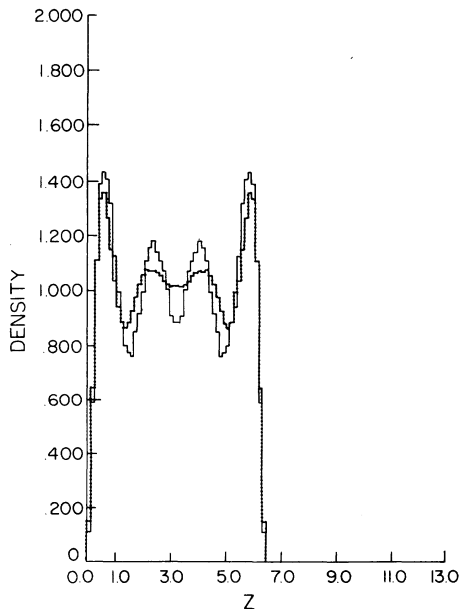


FIG. 4. Density profiles for quantum hard spheres for  $\rho a^3 = 0.2$ , and  $L_z = \frac{30}{32} L_{z0}$ . The solid line for  $n_J(z)/\rho$  is from the present treatment. The decorated line for  $n_v(z)/\rho$  is from the variational calculation.

dependence of structure on the channel separation, can hardly be seen, since the structure of this density profile is already damped out considerably. This seems to suggest that the variational wave function used in paper II though correct for the over-all structure fails to describe some subtle but significant correlations properly.

In view of the layered structures developed in these systems and discrepancies between variational treatment and the present "exact" treatment, we have tried to carry out a new set of variational calculation in which we put into  $h(z)$  an explicit oscillatory component,

$$h(z) = h_0(z) [1 + A \cos k(z - \frac{1}{2} L_z)], \quad (13)$$

where  $h_0(z)$  is defined in Eq. (7c). By varying the new variational parameters  $A$  and  $k$ , we were not able to detect any significant lowering of the energy. This is not surprising because the  $h(z)$  in Eq. (13) tends to increase the kinetic energy. This and our previous calculation strongly suggest that one needs a much more complicated trial function to describe these subtle correlations found in the present calculation.

That our structure is not a crystallization effect is verified by an explicit calculation of the distribution of atoms in a plane for a quantum crystal. This distribution can easily be obtained from the crystal configurations obtained in I. We find that this distribution contains regions where the density is essentially zero. This result holds even for individual configurations and arises simply because the atoms are quite well localized on lattice sites. A similar calculation performed for the fluid in the channel generates a completely random distribution of atoms in any one layer. This distribution is also found for individual configurations. We thus believe that there is no evidence of any crystallization phenomena taking place in the layers in the channel.

Finally we remark that the structure we have found in our exact treatment of a fluid Boson system, is qualitatively similar to that predicted by Regge<sup>7</sup> in a recent publication on the free surface of a Boson fluid. Indeed, he pointed out that his method when applied to a channel would yield an oscillatory density profile. We have not attempted a quantitative comparison of his results and our own.

We shall discuss this layered structure in more detail in Sec. VI.

#### IV. COMPARISON WITH CLASSICAL HARD SPHERES

The pronounced layered structure we found for quantum hard spheres suggested that we should carry out Monte Carlo calculations for a classical

hard sphere<sup>8</sup> system in a channel. We chose to model a system with density  $\rho a^3 = 0.7$ . The density has approximately the same ratio (0.74) to the freezing density of classical hard spheres as  $\rho a^3 = 0.2$  (the density used in our boson systems) does to the quantum freezing density (0.23). In Fig. 5 we give the density profile for 64 particles in a channel bounded by two rigid walls. We see a qualitatively similar layered structure to the one we found in the quantum system, except of course that the density is peaked at the walls for the classical system. A series of calculations in which the channel width was varied from  $\frac{3}{4}$  to  $\frac{5}{4}$  of the one shown in Fig. 5, yielded similar density profiles with layered structures, but the number of layers changed from four to five to six layers successively. Similar calculations were carried out for the  $\rho a^3 = 0.5$  case, where a layered structure as well as the dependence of the number of layers on the channel width was again observed. This shows that the layered structures exist at lower density as well. The relationship between the channel spacing and the number of layers is summarized in Table I. This kind of density oscillation has also been reported for a model of a one-dimensional fluid near a rigid surface.<sup>9</sup>

#### V. STABILITY OF LAYERED STRUCTURES

As a test of convergence we use the idea that if a system has reached stable (*not metastable*) equilibrium, then if it is disturbed, it should

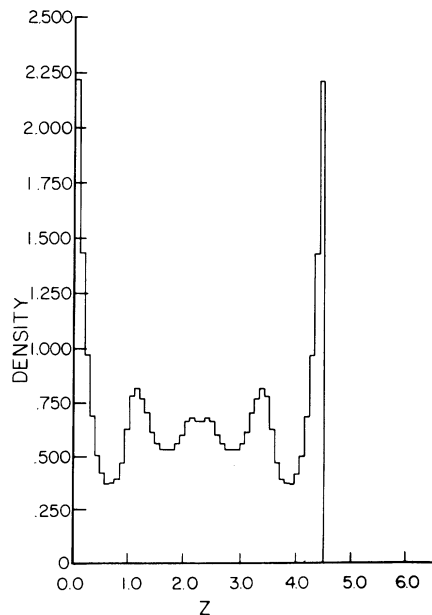


FIG. 5. Density profiles for classical hard spheres in a channel for  $\rho a^3 = 0.7$ , and  $L_z = 4.505 a$ .

always come back to the same equilibrium state. To disturb a system in the context of our present calculations, we force the equilibrium state into a new state. Then if the calculations are started from the new state, we should ultimately find the same equilibrium state from which we started.

For the quantum hard-sphere system, we took pains to verify that equilibrium can be restored after a violent disturbance for the case  $L_{z1} = L_0$ . The starting distribution was derived from a calculation of classical hard spheres which gives the density profile shown in Fig. 5. After re-scaling the box size to give the desired average density, Eq. (6) was iterated with this distribution as an initial input. After about 600 iterations for a population of approximately 300 configurations the system readjusted itself to the equilibrium state we found previously. For comparison, the density profiles in Figs. 2-4 are the results of 1000, 500, and 500 iterations, respectively, for about the same number of configurations. Thus, when we start from a very bad initial state, relaxation to equilibrium is very slow.

For the classical hard spheres, the starting configuration was obtained by imposing an external potential to force the particles to accumulate near the center of channel in a highly localized state. In less than half a million configurations, the recovery to the previous (equilibrium) state was complete.

#### VI. DISCUSSION

The main points that our calculations have revealed are:

(i) In an exact treatment of a fluid Boson system confined in a channel with ridged walls, we find a very pronounced layered structure across the channel.

TABLE I. Dependence of number of layers  $m$  on the channel width  $L_z$  for classical hard spheres in a channel at two densities,  $\rho a^3 = 0.5$  and  $0.7$ .

| $\rho a^3$ | $L_z/a$ | $m$ |
|------------|---------|-----|
| 0.7        | 3.38    | 4   |
|            | 3.66    | 4   |
|            | 3.94    | 5   |
|            | 4.22    | 5   |
|            | 4.51    | 5   |
|            | 4.79    | 5   |
|            | 5.07    | 6   |
| 0.5        | 5.63    | 6   |
|            | 3.78    | 4   |
|            | 4.10    | 5   |
|            | 4.41    | 5   |

(ii) A similar but much less pronounced structure is known to be a feature of variational calculations.

(iii) The layered structure found in the exact calculations is very sensitive to the channel width: the number of layers changes abruptly as the channel width is changed.

(iv) All the general features that are present in the exact quantum treatment are also present in a classical system of hard spheres confined in a channel.

Since the classical calculations are comparatively quick to perform, we have studied this system in considerable detail to try to elucidate the behavior of the system. We found two further striking features.

(v) The number of layers present in the channel is semiquantitatively related to the oscillations in the radial distribution function for a bulk system of hard spheres at the same density. The relationship can be stated in the following way. As the channel width is increased, a new layer appears whenever the channel is just wide enough to accommodate  $m$  layers (peak to peak), a distance  $l$  apart. Here  $l$  is the peak to peak spacing of the oscillations in the distribution function  $g(r)$ .

(vi) As the channel width is increased beyond the point at which a new layer appears, the layered structure remains stable, the central peaks broadening to maintain a constant number of layers, the outer peaks remain comparatively unchanged both in width and height. No new layer appears until the channel has widened by an amount  $l$  defined in (v) above. These results were obtained by studying a classical system as the number of layers changed from four to five and from five to

six.

Turning now to the quantum system, we have tested the results stated in (v) and (vi) for the transition from four to five layers and the transition from five to six layers. We find that both results are well verified, showing once again that the quantum and classical hard-sphere systems behave in a strikingly similar manner at the correctly scaled densities.

These results can be summarized in the following way. As the channel is widened, and new material added to the system to maintain constant density, the system adjusts so that the total number of layers remains fixed and the central peaks are broadened. We speculate that this phenomena may be very important in understanding the behavior of thin films of liquid helium bound to a substrate. If we are allowed to interpret the free surface as providing a boundary condition on the system, then after  $m$  layers are complete if additional material is added then it may not form an additional partial layer but the whole system may adjust by thickening some of the interior layers and maintaining the total number of layers constant until the total thickness of the film is such that an extra layer can be accommodated.

#### ACKNOWLEDGMENTS

We want to thank Dr. L. Verlet and Dr. D. Levesque for kindly supplying us with a copy of their Monte Carlo code for hard spheres in a uniform system. Our calculations used a modification of their program. Of course, we alone are to be blamed for any possible errors in our code.

\*Work supported by the U. S. AEC under Contract No. AT(11-1)-3077 and by the National Science Foundation under Grant No. GH-36457.

†Present address: New York University, Courant Institute, 251 Mercer Street, New York, N. Y. 10012.

<sup>1</sup>F. D. M. Pobell, H. W. Chan, L. R. Corruccini, R. P. Henkel, S. W. Schwenterly, and J. D. Reppy, *Phys. Rev. Lett.* **28**, 542 (1972); I. Rudnick, and J. C. Fraser, *J. Low Temp. Phys.* **3**, 225 (1970); D. F. Brewer, *J. Low Temp. Phys.* **3**, 205 (1970); W. D. McCormick, D. L. Goodstein, and J. G. Dash, *Phys. Rev.* **168**, 249 (1968); and earlier works quoted in these papers. For more recent experiments, see *Monolayer and Submonolayer Helium Films*, edited by J. G. Daunt and E. Lerner (Plenum, New York, 1973).

<sup>2</sup>D. F. Brewer, in Ref. 1.

<sup>3</sup>V. L. Ginzburg and L. P. Pitaevskii, *Zh. Eksp. Teor. Fiz.* **34**, 1240 (1958) [*Sov. Phys.-JETP* **1**, 858 (1958)]; E. P. Gross, *Nuovo Cimento* **20**, 454 (1961).

<sup>4</sup>M. H. Kalos, D. Levesque, and L. Verlet, *Phys. Rev. A* **9**, 2178 (1974).

<sup>5</sup>K. S. Liu, M. H. Kalos, and G. V. Chester, *J. Low Temp. Phys.* **13**, 227 (1973).

<sup>6</sup>M. H. Kalos, *Phys. Rev. A* **2**, 250 (1970).

<sup>7</sup>T. Regge, *J. Low Temp. Phys.* **9**, 123 (1972); and (private communication).

<sup>8</sup>N. Metropolis, A. W. Rosenbluth, M. N. Rosenbluth, G. H. Teller, and E. Teller, *J. Chem. Phys.* **21**, 1087 (1953).

<sup>9</sup>See, for example, I. Z. Fisher, *Statistical Theory of Liquids* (Univ. of Chicago Press, Chicago, Ill., 1956).